Left frontal white matter atrophy links to timing mechanisms relevant for apraxia of speech

[1, 2]Rose Bruffaerts, MD, PhD, [1]Jolien Schaeverbeke, PhD, [3]Manon Grube, PhD, [1]Silvy Gabel, MSc, [2]An-Sofie De Weer, MSc, [2]Eva Dries, MSc, [2]Karen Van Bouwel, MSc, [3]Timothy D Griffiths, MD, PhD, [4]Stefan Sunaert, MD, PhD, [1,2]Rik Vandenberghe, MD, PhD

[1]Laboratory for Cognitive Neurology, Department of Neurosciences, KU Leuven, Belgium; [2]Neurology Department, University Hospitals Leuven, 3000 Leuven, Belgium; [3]Institute of Neuroscience, Medical School, Newcastle University, Newcastle-upon-Tyne, UK; [4]Radiology Department, University Hospitals Leuven, 3000 Leuven, Belgium.

Corresponding author: Rose Bruffaerts, MD, PhD, Herestraat 49, 3000 Leuven, Belgium, rose.bruffaerts@kuleuven.be

Search terms: primary progressive aphasia, apraxia of speech, nonfluent variant, MRI, rhythm perception

The authors declare no competing financial interests.

Funding: This work was supported by Federaal Wetenschapsbeleid [Belspo 7/11]; FWO [G0925.15] and KU Leuven [OT/12/097, C14/17/108]. RB is a postdoctoral fellow of the Research Foundation Flanders (FWO).

Abstract

Objective

In some patients with apraxia of speech (AOS), we observed impaired perceptual timing abilities, which lead us to propose a shared mechanism of impaired perceptual timing underlying impaired rhythm discrimination (perceptual processing) and AOS (motor speech output). Given that considerable white matter damage is often observed in these patients, we here investigate whether white matter changes are related to impaired rhythm processing as one possible mechanism underlying AOS.

Methods

We applied deformation-based morphometry (DBM) and diffusion tensor imaging (DTI) in 12 patients with the nonfluent variant (NFV) of Primary Progressive Aphasia (PPA) with AOS, as well as 11 patients with the semantic variant and 24 controls.

Results

Seventy-five percent of the patients with NFV displayed impaired rhythm processing and the severity of their impairment correlated with their degree of AOS. Moreover, left frontal white matter volume loss adjacent to the supplementary motor area (SMA) correlated with impaired rhythm processing. In addition, we obtained tract-based metrics of the left Aslant tract, which is typically damaged in NFV. The structural integrity of the left Aslant tract also correlated with rhythmic discrimination abilities in NFV.

Conclusions

Our data suggest that a shared white matter substrate adjacent to the SMA contributes to impaired rhythm perception and motor speech impairments. This indicates that impaired perceptual timing may be one of the neurocomputational mechanisms underlying AOS. Our

observation that regional variations in left frontal lobe atrophy are linked to the phenotypical heterogeneity in NFV may lead the way for earlier diagnosis.

Introduction

The nonfluent variant of Primary Progressive Aphasia (NFV) is characterized by apraxia of speech (AOS) or agrammatism and impaired sentence comprehension[1–3]. NFV is phenotypically heterogeneous: impaired AOS and agrammatism can arise in combination or isolation and hence give rise to three possible subtypes: primary progressive apraxia of speech (ppAOS), progressive agrammatic aphasia or mixed agrammatism and AOS[4–7]. This clinical heterogeneity suggests a diversity of underlying neuroanatomical substrates. The present work focuses on the in-depth characterization of the mechanism and substrate underpinning AOS. Previously, grey matter atrophy has been consistently found in NFV in the left opercular part (BA44) of the inferior frontal gyrus (IFG), insula, premotor and the supplementary motor areas (SMA)[1,8]. Involvement of the SMA and the left lateral superior premotor cortex is linked to ppAOS[4,9,10]. In the ppAOS phenotype, more focal neurodegeneration of the (pre)motor cortex was observed compared to widespread atrophy extending to the frontotemporal regions in progressive agrammatic aphasia[6,7].

Neuropathologically, NFV is somewhat heterogeneous, with a dominance of tau pathology in up to 88% of patients (either Progressive Supranuclear Palsy (PSP), Corticobasal degeneration (CBD) or Pick's disease) and otherwise TDP43 proteinopathy or Alzheimer's disease[11–14]. Frontal white matter changes are more common in NFV caused by tauopathies[15], especially in CBD[16]. At present, in-depth knowledge about the relation between phenotype, structural changes and neuropathology are lacking, whereas a better understanding of this relationship is necessary for targeted development of pharmacological therapy and the implementation of potential clinical trials. So far, neuroimaging studies have mainly focused on grey matter changes. It has been postulated that also white matter changes will contribute to the NFV phenotype, for instance to executive dysfunction[17] or impaired speech production[18,19]. Here, we specifically test whether white matter changes in NFV relate to impaired non-linguistic

processing using non-verbal rhythmic auditory stimuli which do not convey meaning. This is motivated by our previous finding that processing of short sequences of auditory stimuli, more specifically the discrimination of metrical sequences, is significantly impaired in NFV[20]. Because impaired rhythm discrimination co-occurs with AOS, we hypothesized that both deficits are related through a common impairment in a "temporal scaffolding mechanism", which structures input and output in time[20,21]. Consistent with this finding, grey matter atrophy in the left SMA and in the right caudate was associated with impaired performance on a temporal regularity task using spoken syllables[22]. However, prior studies were not designed to evaluate the possible contribution of white matter damage.

In the current study, we have expanded our previously published dataset[20] to now include 12 NFV patients who received auditory testing and volumetric imaging. By focusing on white matter abnormalities, we aim to elucidate the neuroanatomical correlate of the hypothesized temporal scaffolding mechanism. This will aid us in understanding the neurocomputational abnormalities which give rise to AOS. We investigate a correlation between rhythm perception deficits and tensor-based deformations of the whole brain (deformation-based morphometry, DBM) and diffusion tensor imaging (DTI). In the current study, we opted for DBM rather than voxel-based morphometry (VBM) because automated segmentation in regions of abnormal grey and white matter might be unreliable and because DBM in addition allows visualization of changes in subcortical structures containing grey and white matter[23]. Furthermore, we complement DBM with DTI. DTI is sensitive to white matter damage caused by tau pathology, which frequently underlies the NFV phenotype[24,25]. We focused on the left frontal Aslant tract, which connects BA44 to medial frontal areas including the SMA[26]. Damage of the left Aslant tract is considered specific for the NFV phenotype[19,27]. Because it connects IFG with SMA, which has been previously identified as a gray matter correlate of temporal regularity processing in NFV[28], the left Aslant tract might also play a role in temporal scaffolding. Our

approach aims to clarify the relationship between AOS, rhythm discrimination and their potentially overlapping anatomical substrate to elucidate the phenotypical heterogeneity in NFV.

Methods

Participants

The study was approved by the Ethics Committee, University Hospitals Leuven. All participants provided written informed consent in accordance with the Declaration of Helsinki. PPA patients were recruited via the memory clinic University Hospitals Leuven. A consecutive series of 38 patients who fulfilled the international consensus criteria for PPA[1] enrolled for the experiment (2011-2019). The first 23 patients are the cohort which was described in [20], and the same case numbers will be used for consistency. Seven of the 38 patients had to be excluded for the following reasons: hearing loss (n = 3); lack of ability to perform the experimental tasks according to practice runs due to disease severity (n = 2); lack of cooperation (n = 1); unique phenotype (foreign accent syndrome, n = 1). The remaining 31 patients were able and sufficiently cooperative to undergo the extensive psychoacoustic testing and produce reliable data. Before the study, each patient was classified according to the 2011 recommendations[1]. The classification relied on the clinical evaluation by an experienced neurologist (R.V.), in combination with neurolinguistics assessment and clinical MRI, as well as, where available, [^{18}F]fluorodeoxyglucose PET ([^{18}F]-FDG PET), CSF biomarkers for Alzheimer's Disease and [^{11}C]-Pittsburgh compound B amyloid PET. Twelve cases were classified as NFV (Table 1), 11 as the semantic variant of PPA (SV), and 8 as the logopenic variant (LV). The LV group will not be discussed further because of the smaller sample size compared to the NFV and SV groups. Of the 12 NFV cases, all exhibited AOS on clinical examination and 5 patients (case

20-23 and 31) also displayed single-word comprehension deficits upon testing and would also fit the more recently described criteria for the "mixed variant"[2,29]. All patients received a volumetric MRI scan and 7 NFV and 7 SV DTI imaging. Twenty-nine healthy controls (15 male, age range 51-76, education range 9-22 years) underwent psychoacoustic testing, 24 of these controls received volumetric MRI and 20 DTI imaging. Hearing sensitivity was measured in all participants using a clinical Bekesy-type audiometer for frequencies of 0.5, 1, 2, 4 and 8Hz, on the left and right ear, respectively. In the pure-tone audiograms, all participants were able to detect stimuli of up to 1000 Hz below a hearing level of 30 dB on at least one side.

Behavioral testing

Neuropsychological testing consisted of confrontation naming by means of the Boston Naming test using Dutch Norms. Non-verbal executive functioning was evaluated by means of the Raven's Coloured Progressive Matrices. Repetition was assessed using the Akense Afasie test. To assess AOS, the Diagnostisch Instrument voor Apraxie van de Spraak (DIAS) was added to the cognitive test battery when it became available (for this reason it was not performed in cases 6, 13, 15 & 21). The DIAS consists of vowel and consonant repetition (15 trials each) and diadochokinesis testing. During the latter task, the examiner first reads three successive alternating syllables aloud, e.g., "pa ta ka" and asks the patient to repeat these once. If the patient was able to repeat this sequence correctly, he/she was asked to repeat it as many times as possible during a period of 8 s. The diadochokinesis severity score is then the total sum of correctly repeated syllables in this period. Grammaticality was assessed using the auditory sentence comprehension test of the Werkwoorden en Zinnen Test (WEZT). This test consists of 40 sentence-picture matching trials, using active or passive sentences with possible role reversal (e.g. "the horse was kicked by the cow").

Rhythm perception

The psychoacoustic testing session comprised 4 pre-existing tasks of perceptual rhythm and timing (r1-r4)[20](Fig 1). The rhythm tasks followed a two-alternative forced choice algorithm. Depending on preference and ability, participants responded verbally or by pointing to a graphical scheme showing the possible options. Instruction, verbally and graphically, were repeated until the subject confirmed they understood the task. Five practice trials were repeated until five consecutive correct responses were recorded, and if needed, instructions were repeated and the nature of the errors was explained. If the subject indicated during the test phase that they had forgotten the instructions, the instructions were repeated, the practice trials run again and the test phase then restarted.

All tasks used 500 Hz 100 ms pure tones. Outcome measures were the thresholds obtained by adaptively adjusting the difference between reference and target stimuli. The difference was varied as a relative proportion of the duration or tempo of the reference. The basic 'Single time-interval duration discrimination' task (r1) required participants to indicate which of two tone pairs comprised the 'longer gap' than the reference of varying duration (inter-onset interval of 300–600 ms). In the 'Isochrony deviation detection' task (r2; 50 trials), participants were required to indicate which of two otherwise isochronous five-tone sequences contained a lengthening or 'extra gap'. The reference sequence had an isochronous interonset interval ranging from 300 to 600 ms, the target had one lengthened interonset interval between the third and fourth tone. In the 'Metrical pattern discrimination' tasks (r3, r4; 50 trials), participants were required to decide which of three rhythmic sequences (the second or the third) of seven tones each sounded 'different', or 'wrong', based on a distortion (or change) in the rhythm. The reference sequence had a strongly (r3) or a weakly (r4) metrical beat of 4.

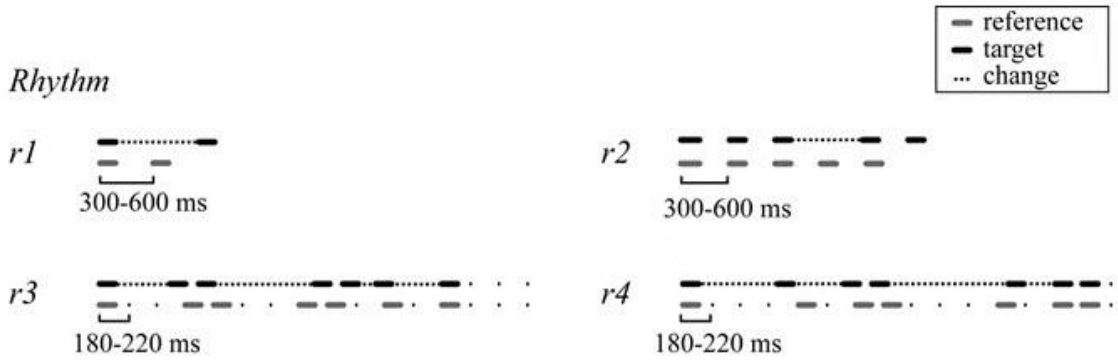

Figure 1 Perceptual timing tasks.

Statistical analysis

The analysis of the rhythm tasks was identical to the procedure we have described in prior work[20]. Outcome measures were log-transformed to allow for parametric analysis at the group level. At the individual level, each PPA patient's performance was analyzed in comparison to the group by using a modified Crawford t-test[30]. For the comparison between each individual patient and the controls, to facilitate comparison between tasks and to enable Bonferroni correction, the exact P values (estimated percentiles) calculated according to Crawford and Garthwaite were transformed into normalized Z-scores using the standard normal cumulative distribution function. The significance threshold was set to Z = 2.24 equaling a one-tailed significance level of $P<0.05$, Bonferroni-corrected for the number of tests (n = 4). We compared the rhythm test scores between NFV and SV using a Student's *t*-test (one-tailed significance level of $P<0.05$). In 8 NFV, behavioral measures of AOS and grammaticality were obtained. We correlated these measures to the rhythm test scores to evaluate the link between impaired rhythm discrimination and AOS (one-tailed significance level of $P<0.05$).

Acquisition of MRI data

Twenty-three patients (12 NFV and 11 SV), and 24 healthy controls received a high resolution T1-weighted structural MRI. All controls and 13 patients were scanned on a 3 T Philips Intera system equipped with an 8-channel receive-only head coil (Philips SENSitivity Encoding head coil). Ten patients were scanned on a 3T Philips Achieva dstream scanner equipped with a 32-channel head volume coil. For structural imaging, an identical 3D turbo field echo sequence was used on both systems (coronal inversion recovery prepared 3D gradient-echo images, inversion time (TI) 900 ms, shot interval = 3000 ms, echo time (TE) = 4.6 ms, flip angle 8 degrees, 182 slices, voxel size 0.98 x 0.98 x 1.2 mm^3). The diffusion weighted images consisted of 45 directions of diffusion weighting with a b = 800 as well as 1 non-diffusion weighted image (B0), acquired in the axial plane, with isotropic voxel size of 2.2 mm, TR 9900 ms, TE 90 ms, flip angle 90°, fold over direction AP, fat shift direction A (anterior), in-plane parallel image acceleration (SENSE) factor 2.5.

Deformation-based morphometry

DBM was performed using the CAT12 toolbox (Structural brain mapping group, Jena, Germany, http://www.neuro.uni-jena.de/cat), an extension of SPM12 (Wellcome Trust Centre for Neuroimaging, London, UK, http://www.fil.ion.ucl.ac.uk/spm). Segmentation was performed in CAT12 using a default tissue probability map. Local adaptive segmentation was used at default strength (medium) and Diffeomorphic Anatomical Registration Through Exponentiated Lie Algebra (DARTEL) was used for registration to the default template (IXI555_MNI152). Voxel size for normalized images was set at 1.5 mm (isotropic) after internal resampling at 1mm. Local deformations were estimated using the Jacobian determinant, while ignoring the affine part of the deformation field. Thus, additional correction for total intracranial volume is not required[31]. Images were smoothed using a 8 x 8 x 8 mm^3 Gaussian kernel. Deformation fields of healthy controls and both PPA subtypes were compared

using a one-way between-subject ANOVA. Multiple linear regression was used to correlate rhythm tests (r1-r4) at the individual level to local deformations of the grey and white matter within each PPA subtype group. Scanner type and age were introduced as a nuisance variable in all analyses. Threshold of significance was set at voxel-level uncorrected $P<0.001$ and cluster-level FWE-corrected $P<0.05$[20]. To confirm that these changes were related to white matter involvement, a supplementary VBM analysis using segmented white matter maps was performed in which total intracranial volume (TIV) was added as a nuisance variable and the outcome of the DBM analysis was used for small volume correction.

Diffusion Tensor Imaging

Diffusion images were preprocessed and analyzed with MRTRIX3. The preprocessing pipeline included the following steps in order of use: first, the data were converted from DICOM to MIF using mrconvert. Using dwidenoise, diffusion data were denoised; subject motion, eddy current artefacts were corrected for as well using dwidenoise (which relies on FSL eddy); following these two steps, the preprocessed diffusion data were bias-corrected with dwibiascorrect. The diffusion data were rigidly aligned to the subject's T1-weighted volume space using Advanced Normalization Tools (ANTs) and tensor reorientation was performed. Fractional anisotropy (FA) and mean diffusivity (MD) was calculated in subject-space and normalized to MNI space. The calculated tensors were then used to carry out a whole brain tractography using the probabilistic Tensor (Tensor_Prob), combined with anatomically constrained tractography with seeding along the grey/white matter interface, and 2 million streamlines to be selected[32]. The whole brain tractogram was then segmented using volumes of interest (VOIs) acquired from the Freesurfer aparc+aseg parcellation[33,34]. These VOIs were pars opercularis of the IFG and the superior frontal gyrus, specifically selecting the Aslant tract on diffusion MR data[26].

Freesurfer aparc+aseg parcellation was performed to obtain these subject-specific VOIs. For this reason preprocessing of T1-weighted structural MRIs was repeated using FMRIPREP[35,36], a Nipype[37] based tool. T1-weighted volume was corrected for intensity non-uniformity using N4BiasFieldCorrection v2.1.0[38] and skull-stripped using antsBrainExtraction.sh v2.1.0 (using the OASIS template). Brain surfaces were reconstructed using recon-all from FreeSurfer v6.0.1[39], and the brain mask estimated previously was refined with a custom variation of the method to reconcile ANTs-derived and FreeSurfer-derived segmentations of the cortical gray matter[40]. Spatial normalization to the ICBM 152 Nonlinear Asymmetrical template version 2009c was performed through nonlinear registration with the antsregistration tool of ANTs v2.1.0 using brain-extracted versions of both T1-weighted structural MRI and template. Brain tissue segmentation of cerebrospinal fluid, white matter and gray matter was performed on the brain-extracted T1-weighted structural MRI using fast (FSL v5.0.9).

MD and FA were compared between controls and PPA subtypes using a between-subject ANOVA on the smoothed FA and MD maps using the same threshold as before. Scanner type, TIV and age were introduced as a nuisance variables. A template for the left Aslant tract was generated for healthy controls using the 75% overlap threshold[26]. FA and MD of the left Aslant tract were extracted for each PPA patient by averaging values from all voxels included in the template derived from healthy controls[26]. We compared the FA and MD between the NFV and SV by means of a Student's t-test (one-tailed $P<0.05$). FA and MD were correlated to the rhythm test scores within the NFV group to confirm the DBM findings (one-tailed $P<0.05$).

Data availability

The data that support the findings of this study are available from the corresponding author upon reasonable request.

Results

Rhythm perception results

Performance on the rhythm tasks was poorer in NFV compared to controls (Fig 2AB): mean Z scores were above the preset threshold ($P<0.05$ Bonferroni-corrected) in NFV for discrimination of strongly metrical sequences (r3, mean Z: 2.94), discrimination of weakly metrical sequences (r4, mean: 2.93) and isochrony deviation detection (r2, mean: 2.46) (Fig 2B). We compared the rhythm test scores between the NFV and SV. This confirmed worse scores in NFV for the discrimination of weakly metrical sequences (r4, $P = 0.001$) (Fig 2AB), with. A trend was further found for single-time interval discrimination (r1, $P = 0.051$).

At the individual level, deficits were observed mainly in NFV after correction for the number of perceptual timing tasks performed ($Z > 2.24$) (Fig 2C). On the weakly metrical pattern discrimination task (r4), 7 NFV (Fig 2C) and 2 SV were significantly impaired. Similarly, strongly metrical pattern discrimination (r3) was impaired in 6 NFV (Fig 2C) and 4 SV, as well as isochrony deviation detection (r2) in 6 NFV (Fig 2C) and 2 SV patients. Single time-interval discrimination (r1) was impaired in 4 NFV (Fig 2C) and 1 SV patient. In summary, 75% of NFV were impaired in one or more of the rhythm and timing tasks and 36.4% of SV.

Correlation with behavioral measures of speech

A subset of 8 patients with NFV performed specific behavioral tests to quantify the severity of AOS and agrammatism. In these participants, repetition of consonants was more difficult when single time-interval duration discrimination (r1, $r = -0.84$, $P = 0.009$), isochrony deviation detection (r2, $r = -0.73$, $P = 0.040$) and strongly metrical pattern discrimination (r3, $r = -0.75$, P

= 0.032) were weaker. No correlation was found with repetition of vowels or repetition of diadochokinesis. Grammaticality scores were lower when single time-interval duration discrimination (r1, r = -0.81, P = 0.014) and strongly metrical pattern discrimination (r3, r = -0.73, P = 0.039) were impaired. Repetition of consonants was highly correlated with grammaticality scores in our cohort (r = 0.90, p = 0.002).

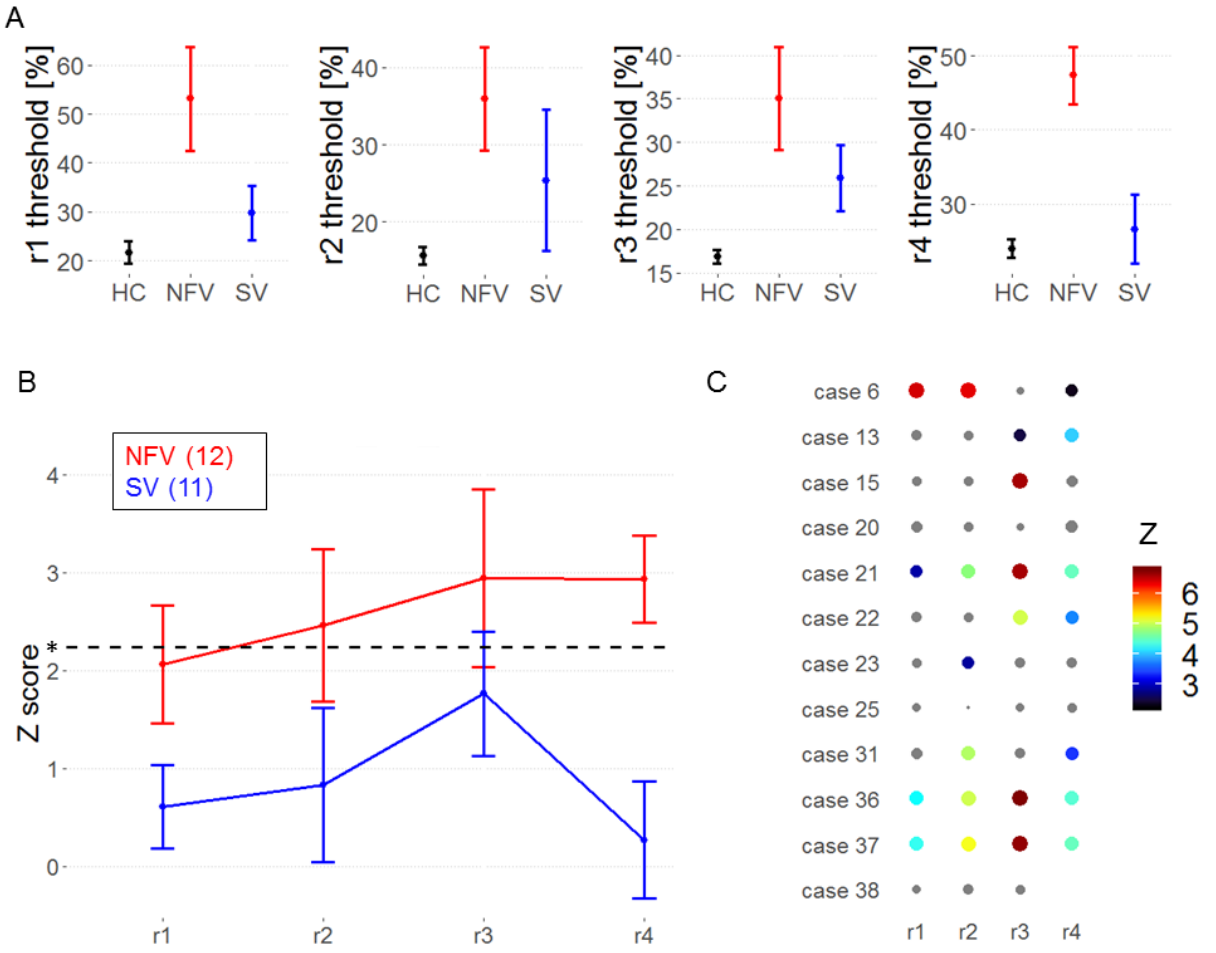

Figure 2 Patients' performance on rhythm perception tasks relative to controls A) Mean raw thresholds and standard error of the mean across controls and PPA subtypes, B) Mean Z scores and standard error of the mean across PPA subtypes. Dotted line represents the Z cut-off for Bonferroni-corrected P<0.05. C) Z-scores of rhythm tests in NFV. Size and color of dots reflect z-score value, non-significant values are gray. Missing data indicates that the patient was unable to perform the task.

White matter changes: Deformation-based morphometry

A comparison between healthy controls and PPA subtypes displayed the expected pattern of changes of the local deformation field. In NFV, loss of volume was observed mainly in the frontal lobes, with left-sided predominance (Fig 3AB). In SV, loss of volume was localized to the anterior temporal lobes (Fig 3A). In the NFV group, voxel-wise multiple linear regression showed that impairment on the strongly metrical rhythm discrimination task (r3) negatively correlated with changes in the deformation field in the left frontal white matter (MNI = -20,20,-36; -17,8,48; -9,39,50; k_E 2426 voxels, Z score: 4.92) (Fig 4AB). This negative correlation indicates that poorer discrimination is linked to more volume loss. For illustrative purposes, we plotted the individual NFV thresholds for the strongly metrical discrimination task (r3) versus volume loss in this region (Pearson's R = -0.316, P < 0.001) (Fig 4C). This loss of volume was more regional than the widespread loss of volume observed at the level of the between-group comparison (Fig 3AB). An additional VBM analysis using segmented white matter maps of the NFV patients confirmed that the loss of volume was related to white matter changes (5 clusters surviving the preset significance threshold, largest cluster: MNI = -8,48,30; k_E 203 voxels, Z = 3.74). In the SV group, DBM analysis yielded no significant correlations with the rhythm test scores.

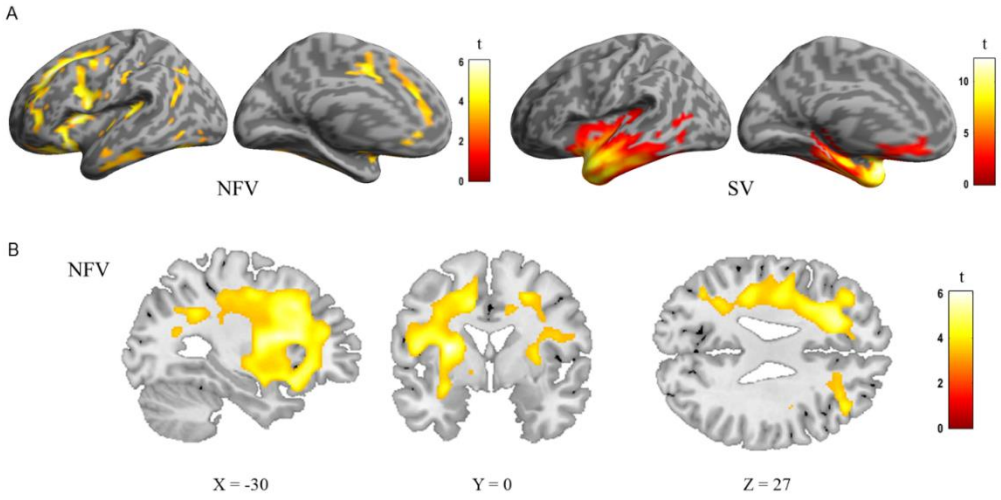

Figure 3 DBM analysis: comparison of controls, NFV and SV. A) Renderings shows deformation of 12 NFV and 11 SV compared to 24 controls (cluster-level FWE-corrected P<0.05). B) Slices in NFV

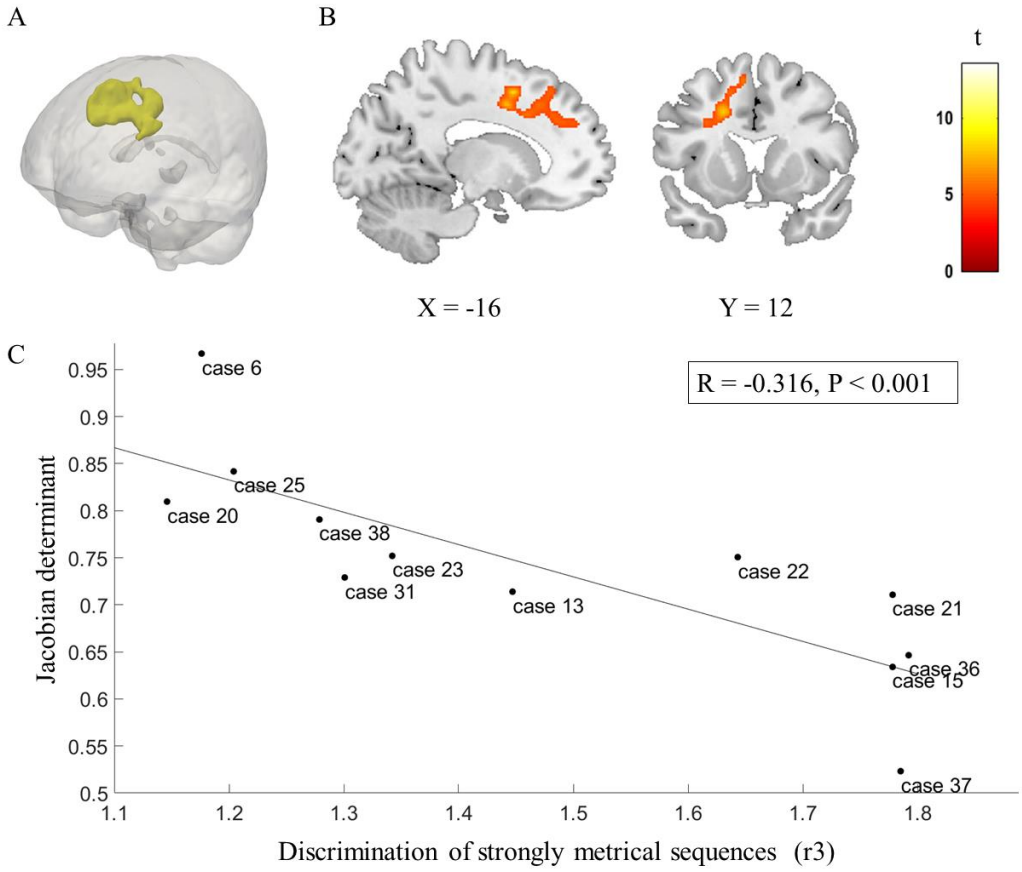

Figure 4 DBM of strongly metrical sequence in NFV. A) Rendering B) Slices C) Correlation between volume loss and strongly metrical sequence thresholds (r3) in NFV patients in the region of interest (AB), exploratory plot for illustrative purposes (case numbers refer to table 1)

White matter changes: Diffusion Tensor Imaging

A comparison between NFV, SV and controls showed reduced FA in NFV in the left inferior frontal region, the corpus callosum and the anterior cingulate (Fig 5A). MD was widely increased in NFV, with a predominance in the both frontal lobes (Fig 5B). In SV, FA was reduced and MD was increased compared to controls in both anterior temporal lobes (not shown). We then compared FA and MD between NFV and SV specifically within the template of the left Aslant tract calculated on 20 healthy controls. FA was similar between NFV and SV ($P=0.175$, Fig 5C). MD was higher in NFV compared to SV ($P = 0.038$, Fig 5D). In NFV, MD in the left Aslant tract was increased when the performance on the strongly metrical rhythm discrimination task was weaker (r3) ($r = 0.815$, $P = 0.026$) and a trend was observed with FA ($r = - 0.708$, $P = 0.075$). FA and MD in the left Aslant tract did not correlate with performance on any other rhythm task in NFV (r1,r2,r4, all $P>0.231$). Visual inspection of the left Aslant tract in NFV showed that this tract overlapped with the region in which also DBM identified white matter volume changes (Fig 5E).

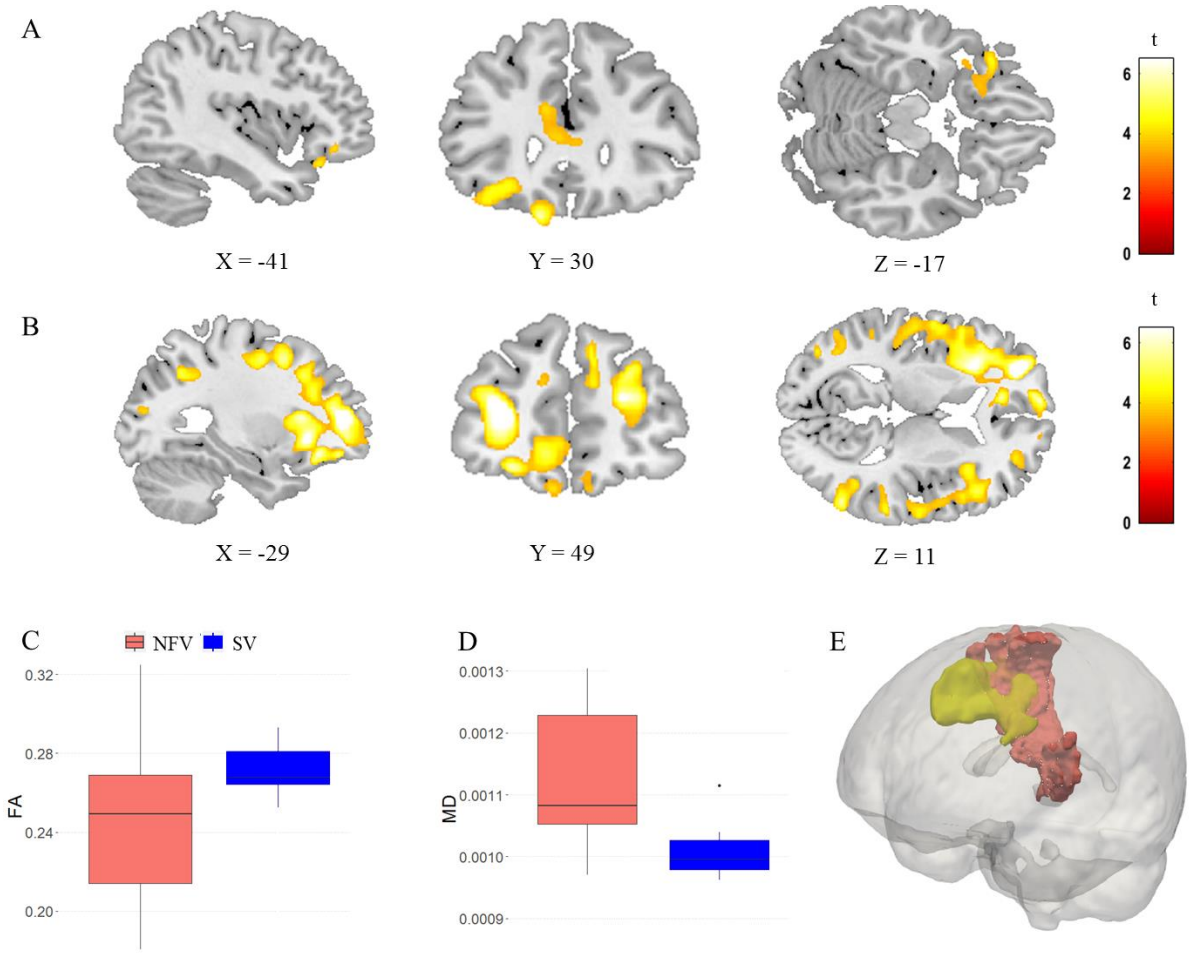

Figure 5 DTI Metrics. A) FA in NFV versus controls (cluster-level FWE-corrected P<0.05). B) MD in NFV versus controls (cluster-level FWE-corrected P<0.05). Comparison of C) FA and D) MD in the left frontal Aslant tract between the NFV and SV subtypes. E) Visualization of the Aslant tract in NFV, based on the 75% overlap of individual tracts in NFV (red) as well as the region of interest derived from DBM (yellow)

Discussion

By investigating whether white matter changes are linked to perceptual timing impairments in AOS, we aim here to elucidate the link between the clinical heterogeneity and structural abnormalities. We proposed a shared mechanism for impaired rhythm discrimination and AOS[20], whereby the impact of disrupted temporal scaffolding might well extend beyond the

linguistic domain. Behaviorally, we here observed a correlation between impaired rhythm discrimination and the degree of AOS. Using DBM, we found atrophy in the left frontal lobe to be correlated with the rhythm discrimination impairment in NFV. We complemented the DBM analysis with DTI in order to provide an independent measure of structural integrity of white matter. Specifically, we focused on the left Aslant tract because this tract has been implicated in motor speech deficits in NFV specifically[19,26,27]. DTI results further confirmed a correlation between damage to the left Aslant tract and impaired rhythm perception in our NFV cohort. Our findings link impaired perceptual timing of incoming non-linguistic auditory signals to degeneration of the left frontal Aslant tract. Given the prior work implicating the left Aslant tract to motor speech production deficits in NFV[19,26,27], we here identify it as a relevant (part of a) common anatomical substrate for impaired rhythm discrimination and AOS. This observation provides additional insight into the neurocomputational mechanism of distorted speech, namely how temporal irregularities are introduced into the spontaneous speech patterns in NFV.

While we used metrical sequences to test rhythm discrimination in NFV[20], impaired regularity discrimination was also observed in NFV using spoken syllables[22]. The observation that impaired regularity discrimination in NFV also applies to syllables was viewed by the authors as additional support for the hypothesis that a disrupted generic temporal scaffolding mechanism would also have an impact on linguistic processing in NFV. Here, we observed a concrete shared white matter substrate, the left frontal Aslant tract, which might contribute to impaired rhythm perception as well as motor speech impairments. In particular, our DBM findings locate the relevant white matter degeneration in the left frontal Aslant tract close to the SMA, which was previously linked to temporal regularity discrimination[41] and AOS[6,9]. The Aslant tract connects the superior frontal gyrus/SMA to IFG, the region which displays the most pronounced atrophy in early NFV[42]. Agrammatism has been linked to grey matter damage in

left BA44[43] and white matter damage in the adjacent left anterior inferior and middle frontal regions and uncinate fasciculus[7], which connects IFG to the temporal lobe[18,26]. Greater white matter changes anterior to the motor regions were found in patients with primary agrammatic aphasia compared to patients with both agrammatism and AOS[7]. The close anatomical proximity of IFG and the left Aslant tract could explain why agrammatism and AOS often occur simultaneously in NFV (as evidenced once more by behavioral testing in our cohort), but also why these deficits can occur in isolation[5,44]. Our findings suggest that temporal processing impairment implies white matter involvement of the left frontal Aslant tract adjacent to the premotor regions. Our work about the neurocomputational mechanism of perceptual timing and AOS as such complements the notion that the neuroanatomical substrate of agrammatism is in closer proximity to IFG[6,7,9]. The clinical relevance of our study and related neuroimaging research is that regional variations in left frontal lobe atrophy are linked to the phenotypical heterogeneity in NFV. Some have advocated a fairly strict separation between ppAOS and progressive agrammatic aphasia[4–7]. Evidence for the existence of separate subgroups was also derived from data-driven clustering analysis, which grouped isolated agrammatism as separate group of PPA[44]. Whether lumping AOS and agrammatism into one phenotype or not, a detailed clinical evaluation, namely specifying whether AOS and/or agrammatism occurs in NFV, can be considered useful both from the clinical and scientific viewpoint.

White matter damage is at least part of the underlying cause of impaired rhythm perception and speech apraxia in NFV, which we interpret as a disrupted shared mechanism of temporal scaffolding. We hypothesize that these white matter changes reflect tau pathology. Tau pathology is the most frequently found pathology in NFV[13,14] and white matter abnormalities have been reported extensively in tauopathies. White matter atrophy has previously been linked to behavioural changes in tauopathies[45,46] using VBM. However, even though voxelwise analysis is generally accepted, normalization errors cannot be completely excluded when using

VBM or DBM[47]. For this reason, we complemented our investigations with tract-based statistics from diffusion-weighted imaging. DTI imaging is sensitive to changes caused by tau pathology at the single-subject level[24], presumably because of underlying glial pathology[48], e.g. by severe myelin injury or a change in other structures that create barriers for water diffusion[18]. However, neuropathological data to unequivocally link our findings to tau pathology is lacking in all but 2 patients, nor can we discriminate between the neuropathologically different types of tau pathology, i.e. PSP, CBD or Pick's disease.

In conclusion, left frontal white matter changes were found to correlate with impaired rhythm discrimination in NFV. The left Aslant tract was identified as the anatomical substrate of this impaired temporal scaffolding mechanism. By revealing a shared white matter substrate in temporal processing of auditory input and speech output, we increase the mechanistic understanding of the neurological origin of motor speech impairment, specifically AOS, and provide additional evidence that generic processing impairments explain part of the NFV phenotype.

Acknowledgements

The authors thank Dr. B. Bergmans, Dr. Ch. Swinnen, Dr. A. Sieben and Prof. Y.A. Pijnenburg for the referral of patients.

References

1. Gorno-Tempini ML, Hillis AE, Weintraub S, et al. Classification of primary progressive aphasia and its variants. Neurology. 2011;76:1006–1014.

2. Mesulam M-M, Rogalski EJ, Wieneke C, et al. Primary progressive aphasia and the evolving neurology of the language network. Nat Rev Neurol. 2014;10:554–569.

3. Vandenberghe R. Classification of the primary progressive aphasias: principles and review of progress since 2011. Alzheimers Res Ther. 2016;8:16.

4. Josephs KA, Duffy JR, Strand EA, et al. Characterizing a neurodegenerative syndrome: primary progressive apraxia of speech. Brain. 2012;135:1522–1536.

5. Mesulam M-M, Wieneke C, Thompson C, Rogalski E, Weintraub S. Quantitative classification of primary progressive aphasia at early and mild impairment stages. Brain. 2012;135:1537–1553.

6. Tetzloff KA, Duffy JR, Clark HM, et al. Longitudinal structural and molecular neuroimaging in agrammatic primary progressive aphasia. Brain. 2018;141:302–317.

7. Tetzloff KA, Duffy JR, Clark HM, et al. Progressive agrammatic aphasia without apraxia of speech as a distinct syndrome. Brain. 2019;142:2466–2482.

8. Rogalski E, Cobia D, Harrison TM, et al. Anatomy of Language Impairments in Primary Progressive Aphasia. Journal of Neuroscience. 2011;31:3344–3350.

9. Whitwell JL, Duffy JR, Strand EA, et al. Distinct regional anatomic and functional correlates of neurodegenerative apraxia of speech and aphasia: an MRI and FDG-PET study. Brain Lang. 2013;125:245–252.

10. Utianski RL, Whitwell JL, Schwarz CG, et al. Tau-PET imaging with [18F]AV-1451 in primary progressive apraxia of speech. Cortex. 2018;99:358–374.

11. Josephs KA, Boeve BF, Duffy JR, et al. Atypical progressive supranuclear palsy underlying progressive apraxia of speech and nonfluent aphasia. Neurocase. 2005;11:283–296.

12. Harris JM, Gall C, Thompson JC, et al. Classification and pathology of primary progressive aphasia. Neurology. 2013;81:1832–1839.

13. Rogalski E, Sridhar J, Rader B, et al. Aphasic variant of Alzheimer disease. Neurology. 2016;87:1337–1343.

14. Spinelli EG, Mandelli ML, Miller ZA, et al. Typical and atypical pathology in primary progressive aphasia variants: Pathology in PPA Variants. Annals of Neurology. 2017;81:430–443.

15. Caso F, Mandelli ML, Henry M, et al. In vivo signatures of nonfluent/agrammatic primary progressive aphasia caused by FTLD pathology. Neurology. 2014;82:239–247.

16. Feany MB, Dickson DW. Neurodegenerative disorders with extensive tau pathology: a comparative study and review. Ann Neurol. 1996;40:139–148.

17. Mahoney CJ, Malone IB, Ridgway GR, et al. White matter tract signatures of the progressive aphasias. Neurobiology of Aging. 2013;34:1687–1699.

18. Galantucci S, Tartaglia MC, Wilson SM, et al. White matter damage in primary progressive aphasias: a diffusion tensor tractography study. Brain. 2011;134:3011–3029.

19. Canu E, Agosta F, Imperiale F, et al. Added value of multimodal MRI to the clinical diagnosis of primary progressive aphasia variants. Cortex. 2019;113:58–66.

20. Grube M, Bruffaerts R, Schaeverbeke J, et al. Core auditory processing deficits in primary progressive aphasia. Brain. 2016;139:1817–1829.

21. Bekius A, Cope TE, Grube M. The Beat to Read: A Cross-Lingual Link between Rhythmic Regularity Perception and Reading Skill. Frontiers in Human Neuroscience [online serial]. 2016;10. Accessed at: http://journal.frontiersin.org/Article/10.3389/fnhum.2016.00425/abstract. Accessed November 29, 2019.

22. Hardy CJD, Agustus JL, Marshall CR, et al. Behavioural and neuroanatomical correlates of auditory speech analysis in primary progressive aphasias. Alzheimer's Research & Therapy [online serial]. 2017;9. Accessed at: http://alzres.biomedcentral.com/articles/10.1186/s13195-017-0278-2. Accessed February 19, 2019.

23. Cardenas VA, Boxer AL, Chao LL, et al. Deformation-Based Morphometry Reveals Brain Atrophy in Frontotemporal Dementia. Archives of Neurology. 2007;64:873.

24. Sajjadi SA, Acosta-Cabronero J, Patterson K, Diaz-de-Grenu LZ, Williams GB, Nestor PJ. Diffusion tensor magnetic resonance imaging for single subject diagnosis in neurodegenerative diseases. Brain. 2013;136:2253–2261.

25. Whitwell JL, Schwarz CG, Reid RI, Kantarci K, Jack CR, Josephs KA. Diffusion tensor imaging comparison of progressive supranuclear palsy and corticobasal syndromes. Parkinsonism Relat Disord. 2014;20:493–498.

26. Catani M, Mesulam MM, Jakobsen E, et al. A novel frontal pathway underlies verbal fluency in primary progressive aphasia. Brain. 2013;136:2619–2628.

27. Mandelli ML, Caverzasi E, Binney RJ, et al. Frontal White Matter Tracts Sustaining Speech Production in Primary Progressive Aphasia. J Neurosci. 2014;34:9754–9767.

28. Hardy CJD, Agustus JL, Marshall CR, et al. Functional neuroanatomy of speech signal decoding in primary progressive aphasias. Neurobiology of Aging. 2017;56:190–201.

29. Schaeverbeke J, Gabel S, Meersmans K, et al. Single-word comprehension deficits in the nonfluent variant of primary progressive aphasia. Alzheimer's Research & Therapy [online serial]. 2018;10. Accessed at: https://alzres.biomedcentral.com/articles/10.1186/s13195-018-0393-8. Accessed July 22, 2019.

30. Crawford JR, Garthwaite PH. Comparison of a single case to a control or normative sample in neuropsychology: development of a Bayesian approach. Cogn Neuropsychol. 2007;24:343–372.

31. Gaser C, Kurth F. Manual Computational Anatomy Toolbox - CAT12 [online]. 2019. Accessed at: http://www.neuro.uni-jena.de/cat12/CAT12-Manual.pdf.

32. Jones DK. Tractography gone wild: probabilistic fibre tracking using the wild bootstrap with diffusion tensor MRI. IEEE Trans Med Imaging. 2008;27:1268–1274.

33. Fischl B, van der Kouwe A, Destrieux C, et al. Automatically parcellating the human cerebral cortex. Cereb Cortex. 2004;14:11–22.

34. Desikan RS, Ségonne F, Fischl B, et al. An automated labeling system for subdividing the human cerebral cortex on MRI scans into gyral based regions of interest. Neuroimage. 2006;31:968–980.

35. Esteban O, Markiewicz CJ, Blair RW, et al. fMRIPrep: a robust preprocessing pipeline for functional MRI. Nature Methods. 2019;16:111–116.

36. Esteban O, Blair R, Markiewicz CJ, et al. fMRIPrep: a robust preprocessing pipeline for functional MRI [online]. Zenodo; 2019. Accessed at: https://zenodo.org/record/2597526. Accessed April 23, 2019.

37. Gorgolewski K, Burns CD, Madison C, et al. Nipype: A Flexible, Lightweight and Extensible Neuroimaging Data Processing Framework in Python. Frontiers in Neuroinformatics [online serial]. 2011;5. Accessed at: http://journal.frontiersin.org/article/10.3389/fninf.2011.00013/abstract. Accessed April 23, 2019.

38. Tustison NJ, Avants BB, Cook PA, et al. N4ITK: Improved N3 Bias Correction. IEEE Transactions on Medical Imaging. 2010;29:1310–1320.

39. Dale AM, Fischl B, Sereno MI. Cortical Surface-Based Analysis. NeuroImage. 1999;9:179–194.

40. Klein A, Ghosh SS, Bao FS, et al. Mindboggling morphometry of human brains. Schneidman D, editor. PLOS Computational Biology. 2017;13:e1005350.

41. Hardy CJD, Agustus JL, Marshall CR, et al. Behavioural and neuroanatomical correlates of auditory speech analysis in primary progressive aphasias. Alzheimer's Research & Therapy [online serial]. 2017;9. Accessed at: http://alzres.biomedcentral.com/articles/10.1186/s13195-017-0278-2. Accessed February 11, 2019.

42. Mandelli ML, Vilaplana E, Brown JA, et al. Healthy brain connectivity predicts atrophy progression in non-fluent variant of primary progressive aphasia. Brain. 2016;139:2778–2791.

43. Wilson SM, Dronkers NF, Ogar JM, et al. Neural correlates of syntactic processing in the nonfluent variant of primary progressive aphasia. J Neurosci. 2010;30:16845–16854.

44. Leyton CE, Ballard KJ, Piguet O, Hodges JR. Phonologic errors as a clinical marker of the logopenic variant of PPA. Neurology. 2014;82:1620–1627.

45. Cordato NJ, Duggins AJ, Halliday GM, Morris JGL, Pantelis C. Clinical deficits correlate with regional cerebral atrophy in progressive supranuclear palsy. Brain. 2005;128:1259–1266.

46. Lansdall CJ, Coyle-Gilchrist ITS, Jones PS, et al. Apathy and impulsivity in frontotemporal lobar degeneration syndromes. Brain. 2017;140:1792–1807.

47. Smith SM, Jenkinson M, Johansen-Berg H, et al. Tract-based spatial statistics: Voxelwise analysis of multi-subject diffusion data. NeuroImage. 2006;31:1487–1505.

48. Forman MS, Zhukareva V, Bergeron C, et al. Signature tau neuropathology in gray and white matter of corticobasal degeneration. Am J Pathol. 2002;160:2045–2053.

Tables

Case	**6**	**13**	**15**	**20**	**21**	**22**	**23**	**25**	**31**	**36**	**37**	**38**	**Cut off**
Age	52	79	71	78	72	63	62	57	69	58	80	65	/
Gender	F	F	M	M	F	F	F	F	M	F	F	M	/
Education	17	8	15	17	12	15	12	10	18	12	10	16	/
CPM	31	**24**	**24**	30	**12**	32	31	/	29	**21**	**4**	35	28
Dis. Dur.	2	5	1.5	2.5	2.5	5	2.5	3.5	1.5	4	4	3	/
BNT	58	48	55	48	30	41	46	7	29	52	**27**	57	50
AAT rep 1	28	29	30	29	**26**	30	28	**27**	**20**	28	**14**	30	28
AAT rep 2	**26**	**24**	**21**	30	**28**	30	30	29	30	**28**	**25**	30	29
AAT rep 3	**28**	**22**	29	**28**	**24**	30	30	**28**	29	**28**	**27**	29	29
AAT rep 4	**26**	**23**	30	29	**24**	30	29	**15**	29	28	**14**	30	28
AAT rep 5	**26**	**27**	30	30	**15**	30	28	**17**	28	**23**	**10**	30	28
DS	6	**3**	4	6	**2**	4	5	**3**	7	5	**3**	4	4
DIAS cons	/	/	/	**13**	/	15	**10**	14	**13**	**3**	**0**	15	14
DIAS vow	/	/	/	15	/	15	**14**	**14**	**14**	15	**6**	15	15
DIAS dia	/	/	/	103	/	77	**50**	**24**	115	**48**	**6**	**47**	56
Gramm	/	/	/	**36**	/	**35**	**36**	**29**	**31**	**20**	**11**	38	38
Extrapyr	-	-	+	-	-	+	+	+	+	-	-	-	/
CIT Spect	/	/	/	/	/	/	/	+	/	/	/	/	/
Tau CSF	/	312	/	195	**424**	183	/	247	/	298	273	**530**	367
Aβ42 CSF	/	1028	/	816	1060	865	/	1057	/	1320	1264	1139	500
Neuropath	/	CBD	CBD	/	/	/	/	/	/	/	/	/	/

Table 1. Characteristics of NFV patients. Norms were calculated as 2 standard deviations below the mean in the age- and education-matched group of healthy controls (n=29). CPM: Raven's progressive matrices, Dis. Dur.: disease duration (years), BNT: Boston Naming Test, AAT: Akense Afasie Test repetition scores part 1 to 5, DS: digit span forward, DIAS cons: DIAS repetition of consonants, DIAS vow: DIAS repetition of vowels, DIAS dia: DIAS diadochokinesis score, Gramm: grammaticality score WEZT, Extrapyr: extrapyramidal signs upon examination, Neuropath: anatomopathological findings